This article has been accepted for publication in a future issue of this journal, but has not been fully edited. Content may change prior to final publication. Citation information: DOI 10.1109/TASC.2017.2655507, IEEE Transactions on Applied Superconductivity

ASC2016-4EOr3C-06

Progress in development of the superconducting bolometer with microwave bias and readout

Sergey V. Shitov, Artem A. Kuzmin, Michael Merker, Vladimir I. Chichkov, Alexey V. Merenkov, Andrey B. Ermakov, Alexey V. Ustinov and Michael Siegel

***Abstract*—Our new detector and readout concept brings together TES and MKID technologies and exploits the idea of a microwave-induced superconducting transition in a small thin-film micro-bridge. The superconducting transition of the bridge manifests itself as variation in the Q-factor of niobium resonators at 5-8 GHz, somewhat similar to MKID operation. We present data showing the potential for developing this concept into multi-pixel detector arrays. Single-pixel sensitivity was measured at 4.5 K for an input band of 600-700 GHz using a prototype 10 nm-thick Nb bridge of size 1 µm x 500 nm. Radiation from human skin was detected with resolution better than 1K/rtHz, which is encouraging for THz imaging applications. To further improve device sensitivity we are also developing Hf-based devices that operate near 0.35 K. Details about the physics and stability of these devices are discussed.**

***Index Terms*—Terahertz range, superconducting bolometer, transition edge sensor, HEB micro bolometer, electrothermal feedback, high-Q resonator, microwave kinetic inductance detector, FDM readout, microwave bias, superconductor impedance, blackbody calibration.**

I. Introduction

SENSITIVE imaging with superconducting detectors, for example in radio astronomy or public security, can benefit from frequency division multiplexing (FDM), which allows both the most efficient signal integration for each pixel and the reduction of wiring complexity at a cryogenic interface [1]. The FDM technique has been used successfully with superconducting MKID [2] and TES array detectors [3], [4]; their pixels are equipped with individual resonators, which are probed using a comb-spectrum signal sent through a common feed-line. In the case of TES detectors, the probing signal varies due to the thermal resistance effect near the superconducting transition temperature. Both the amplitude and phase variations of the probing signal in an MKID are used to detect the absorption of pair-breaking terahertz photons. A typical MKID resonator ($Q \approx 10^4$) can work at a few gigahertz frequency using relatively inexpensive commercial RF amplifiers; a kilo-pixel MKID array can be integrated on a chip. By contrast, TES detectors usually operate below MHz frequencies due to limitations of a SQUID-based readout. It is difficult to design a fully integrated FDM circuit at such low frequencies.

Can a TES array-detector benefit from GHz-range FDM? At first sight, the answer is negative for at least four reasons: (i) the impedance of a biased TES is relatively high, so a TES cannot replace the MKID in a high-Q resonator; (ii) electro-thermal feedback cannot be designed in the same way as for a traditional TES, (iii) the thermal isolation of an RF resonator made of bulk films is hard to achieve; (iv) the superconducting gap energy, Δ, is nearly zero at the superconducting transition, so the absorption of RF photons does not depend on the number of quasiparticles, thus the impedance cannot be varied. These four general statements are challenged below and in Ref [5-6], where we provide intuitive yet simple physical models of the "RFTES". Below we describe how blackbody radiation was detected using a single-pixel RFTES designed for a 600-700 GHz signal band and a probing frequency of about 5.6 GHz [7].

II. Concept of RFTES detector

A. Equivalent schemes and Q-factor

The simplified scheme of a MKID sensor is presented in Fig. 1(a) using lumped elements; the sensing part is substituted, for simplicity, with a variable (non-linear) resistor, R_{B1}. Since the full current of the resonator is flowing through R_{B1}, reaching a high-Q regime ($Q \approx 10^4$) is possible only at mΩ-resistance values. In Fig. 1(b) an alternative way is presented. To achieve the same Q-factor for two different resonators, they must dissipate equally through their loads R_{B1} and R_{B2} meaning that $I_1^2R_{B1} = I_2^2R_{B2}$. In the case of Fig. 1(b), current through the resonator is split between two branches in proportion $I_2/I_1 = C_2/(C_1 + C_2) \approx C_2/C_R$. Here we assume that $C_2 << C_1 \approx C_R$ and condition of equal Q is $R_{B2} \approx R_{B1}\times(C_1/C_2)^2$. For example, $Q \approx 10^4$ can be achieved either for $R_{B1} = 0.001\ \Omega$ or for $R_{B2} \approx 10\ \Omega$, if $C_1/C_2 = 100$. The case of a quarter-wave distributed resonator is considered in our papers [6], [7]; the value $Q = 7\times10^3$ is achieved experimentally for $R_{B2} \approx 10\ \Omega$. The open-ended section of the resonator plays the role of C_2.

This work was supported by the Ministry of Education and Science of the Russian Federation in the framework of Increase Competitiveness Program of NUST «MISiS» No. K2-2016-051, and from German Federal Ministry of Education and Research 05K13VK4, 13N12025.

Sergey V. Shitov and Andrey B. Ermakov are with the National University of Science and Technology MISiS, Moscow 119049, Russia (e-mail: sergey3e@gmail.com) and with Kotel'nikov Institute of Radio Engineering and Electronics, Russian Academy of Sciences, Moscow 125009, Russia.

Artem A. Kuzmin (e-mail: artem.kuzmin@kit.edu), Michael Merker and M. Siegel are with Institute of Micro- and Nano-Electronic Systems and DFG-Center for Functional Nanostructures (CFN), Karlsruhe Institute of Technology, D-76187 Karlsruhe, Germany (e-mail: michael.siegel@kit.edu).

Vladimir I. Chichkov and Alexey M. Merenkov are with the National University of Science and Technology MISiS, Moscow 119049, Russia (e-mail: chichkov.vladimir@gmail.com).

Alexey V. Ustinov is with the Institute of Physics of the Karlsruhe Institute of Technology, D-76128, Germany and with the Russian Quantum Center, National University of Science and Technology MISiS, Moscow 119049, Russia (e-mail: ustinov@kit.edu).

This article has been accepted for publication in a future issue of this journal, but has not been fully edited. Content may change prior to final publication. Citation information: DOI 10.1109/TASC.2017.2655507, IEEE Transactions on Applied Superconductivity

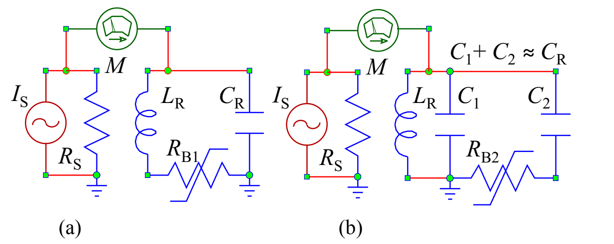

Fig. 1. Equivalent schematics of two high-Q resonators loaded with nonlinear absorbing resistors. The device M must register a minimum of the current from the source R_S at the resonant frequency. (a) The case of a low-resistive absorber R_{B1} (MKID); (b) the partially loaded resonator; the absorber R_{B2} is a higher-resistive RFTES.

B. Variable RF impedance and response

To understand limitations of the impedance variability at high frequencies, the Gorter-Casimir two-fluid model [8] or the Mattis-Bardeen theory [9] can be used. They predict two major effects: (i) the presence of an active impedance for alternating current at temperatures well below T_c, which grows with the photon energy and reaches almost normal state impedance at frequencies comparable with the superconducting energy gap frequency, $f_g=2\Delta/h$ at $T=0$; (ii) reduction of thermal sensitivity, dR/dT, for higher frequencies, as shown in Fig. 2.

The microwave scattering parameters of the layout illustrated in Fig. 3 (left) will be used for further evaluation of the RFTES. The responsivity, S, can be defined as a ratio of the incremental transmission, $\delta|S_{21}|^2$, in the feed-line and the incremental absorption of the incoming signal: $S=\delta|S_{21}|^2/\delta P_{sig}$. The free parameters are the resistance of the absorber, R, and its increment, δR. The conversion efficiency, $\Gamma_H=\delta P_{RF}/\delta P_{sig}=S\times P_{RF}$, can benefit from larger probing power, P_{RF}. The full dissipated power P_{dis} in the bridge is a sum of the signal power and the coupled part of the probing power, which is defined by the parameter $|S_{31}|^2$ and works as a pre-heat. The increment of the total heat, dissipated in the absorber, is $\delta P_{dis}=\delta P_{sig}+\delta|S_{31}(R,\delta R)|^2\times P_{RF}$. The last term in the expression characterizes the electro-thermal feedback and allows different signs of $\delta|S_{31}|^2$: $(\mathrm{sgn}(\delta|S_{31}|^2)=-\mathrm{sgn}(R-R_{emb})$. Since RFTES is a power-to-power converter, the conversion efficiency can be expressed as $\Gamma_H=P_{RF}\times\delta|S_{21}|^2/(\delta P_{dis}-\delta|S_{31}|^2\times P_{RF})$. It is worth adding here that the conversion efficiency Γ_H may turn into gain for $R<R_{emb}$. The gain can grow infinitely until the stability condition $\delta P_{dis}-\delta|S_{31}|^2\times P_{RF}>0$ is true. Such gain may exist even for the relatively smooth dependence $R(T)$ from Fig. 2. We conclude that the regime with gain can be set using a combination of P_{RF} and the bath temperature $T_{bath}<T_c$, (Fig. 3 - right), at least following the above model.

C. Thermal isolation of RFTES detector

In a typical TES-bolometer, the absorber and the thermometer are thermally integrated and isolated from the bath using a suspended dielectric membrane. The electrical connection of the thermometer may limit FDM frequency due to excess reactance of the long wires. Moreover, the size of the absorbing membrane must be larger than the wave length, $\sim\lambda\geq 300$ µm for a THz-signal, which makes it susceptible to the cosmic rays (high-energy particles). An alternative solution, exploiting the superconducting transition, is the nano-volume antenna-coupled HEB, which is based on the hot-electron effect at low temperatures, when electrons are well decoupled from the lattice [10], [11]. Following the nano-HEB concept, RFTES, similarly to MKID, does not need a thermally isolated resonator.

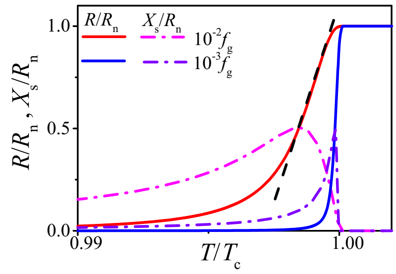

Fig. 2. Real and imaginary components of the impedance calculated from the two-fluid model [8] for a Nb film at frequencies $10^{-2}f_g$, and $10^{-3}f_g$. The dashed line approximates the thermal sensitivity $TdR/RdT\approx 200$ at $f=10^{-2}f_g$.

III. Experimental Details

A. Layout of RFTES detector

Our electromagnetic demonstrator of the RFTES concept [5] is designed for $T_{bath}\approx 4.2$ K. The resonator and the rest of the circuit, except the bridge, are made from 200-nm thick niobium film ($T_c\approx 9$ K) on the sapphire substrate [6], [7]. The embedded micro-bridge is 1.0×0.5 µm^2 and was fabricated from a 10 nm-thick niobium film ($T_c\approx 5.3$-5.8 K) using e-beam lithography and Ar^+ ion-beam etching. The interface between the two layers of Nb is cleaned in-situ with Ar^+ gun. The simplified drawing of the chip with the resonator, the planar antenna and the embedded micro-bridge is presented in Fig. 3. The exact position of the micro-bridge within the resonator (port 3) depends on R_{emb} as described above.

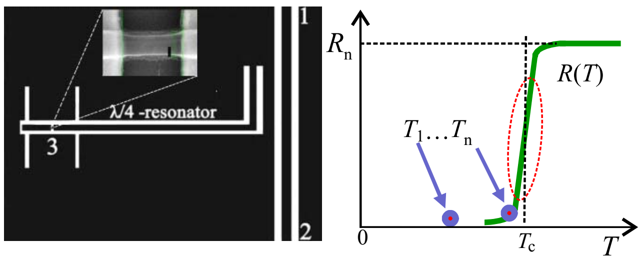

Fig. 3. Simplified layout of the RFTES chip (left). The chip comprises the micro-bridge integrated with the planar resonator and the double-slot antenna. Numbers are: 1 and 2 - input and output ports of the chip, 3 - absorber port is a narrow bridge in series with the central wire of the resonator (a photo of the experimental bridge is shown as the inset). Transfer coefficients S_{21} and S_{31} in the text are for the feed-line and bolometer ports respectively; more details on layout can be found in [6]. The operational points at different bath temperatures $T_1\ldots T_n$ are illustrated on the right.

B. RF probing/biasing

The experimental data on $|S_{21}|^2(f)$ (Fig. 4) illustrates that the micro-bridge in the resonator may abruptly leave its superconducting state as discussed in [6] and [7]. Our analysis suggests that such an event corresponds to the RF current reaching the critical value measured at DC with an accuracy of

This article has been accepted for publication in a future issue of this journal, but has not been fully edited. Content may change prior to final publication. Citation information: DOI 10.1109/TASC.2017.2655507, IEEE Transactions on Applied Superconductivity

±0.5 dB. At this point, we suppose, a hot-spot, i.e. a resistive domain appears across the micro-bridge [12]. It introduces steady losses, which can be seen as a cratered resonance dip. The higher the input microwave power P_{RF}, the bigger the size of the resistive domain and the shallower the dip of $|S_{21}|^2(f)$. The fact that the shape of the crater is reproducible at a given P_{RF} and bath temperature T_{bath} means that the resistive domain is stable and shows no thermal runaways. The stability can be explained by the presence of electrothermal feedback (ETF), very similar to traditional TES [3], or a superconducting antenna-coupled hot-spot micro-bolometer [13]. Substituting a shunt resistor, R_{sh}=R_{emb} , we may conclude that ETF in RFTES devices generally works in the same way as it does in a classical TES.

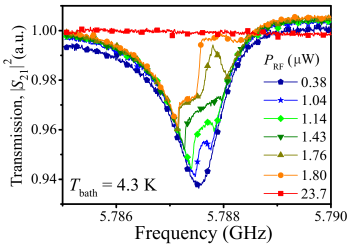

Fig. 4. Non-linear effect (switching) in the optically coupled RFTES detector near the resonance. The probing microwave power, P_{RF}, is a parameter. P_{sig}=0.

C. *Optical off-cryostat detection*

Our initial model of the variable Q-factor includes both the effect of a growing resistive domain in the micro-bridge and the presence of electron-gas heating. Although the electron-gas heating is hard to expect above T > 1 K, the blackbody experiments performed in-situ at T_{bath} ≈ 1.5 K have brought interesting results [7], so we tested the same sample in an optical 4-K cryostat. The synthesized RF generator (see Fig. 5a) provides probing/biasing of the Nb micro-bridge at 5.7875±0.0025 GHz; the immersion sapphire lens focuses the chopped blackbody radiation at the double-slot antenna (Fig. 3); the low-noise amplifier (LNA) provides the proper power level and SNR for homodyne detection with the IQ-mixer and further lock-in registration. The response on the probing microwave power, P_{RF}, is presented in Fig. 5b for blackbody sources with 3 different temperatures. These maxima correspond to peaks of the gain, Γ_H, that must be at maximum of dR/dP_{sig} expected at about the middle of the slope of $R(T)/R_n$ (see Fig. 2). The shifts of the optima are *monotonic* with respect to the temperature of the blackbody. The high gain Γ_H is useful to suppress the noise of the readout electronics at low signal levels. To preserve the dynamic range for large signals, the ETF can be enhanced using greater microwave bias power P_{RF}.

D. *Array RFTES detector*

The array of long resonators is not an easy object for packing within the limited area of the chip. We design and tested the hexagonal package (Fig. 6 left), which can be used with an immersion lens forming the multi-beam "pixel" suitable for further hierarchical integration into a larger array. So far it is confirmed (Fig. 6 right) that elements of the array behave the same way as the above single pixel (Fig. 4).

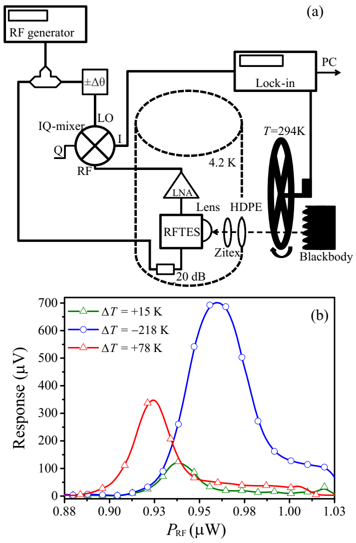

Fig. 5. Optical off-cryostat detection with RFTES at T_{bath} ≈ 4.5 K from Fig. 4: (a) schematic of test setup with the optically chopped blackbody, (b) measured contrast, referenced to the room temperature, 294 K, for various blackbodies at video BW=1 Hz; the blackbodies are liquid nitrogen, boiling water and skin. The measured resolution (noise-equivalent temperature, NET) was better than 1 K at a contrast of +15 K.

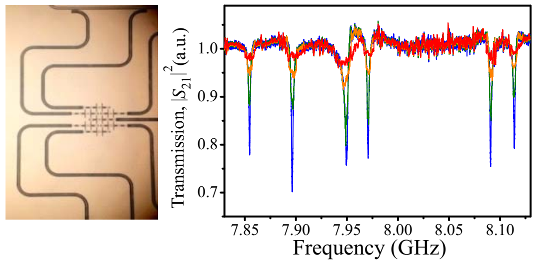

Fig. 6. Hexagonally packed array of 7 RFTES: close-up photo of the chip (left); the experimental spectrum $|S_{21}|^2$ (f, P_{RF}) of the array (right). Color lines are for various probing microwave powers, P_{RF}, similar to Fig. 4. One pixel is missing due to mechanical damage of its resonator.

E. *Material study*

The characteristic energy relaxation times (the quasiparticle recombination time and the phonon escape time) in the thin Nb micro-bridge on sapphire are rather short near T_c ≈ 5.3 K [14]. Thus, the hot-spot regime may dominate in the Nb bridge at T_{bath} ~ 4.2 K. To achieve the hot electron-gas regime, we have developed films of hafnium (T_c= 0.35-0.4 K) as shown in Fig. 7 (left). Such films will be used for the micro-bridges embedded into resonators from Nb. However, the resonance frequencies will be designed to be about 1-2 GHz, to keep the probing frequency at about $10^{-2}f_g$.

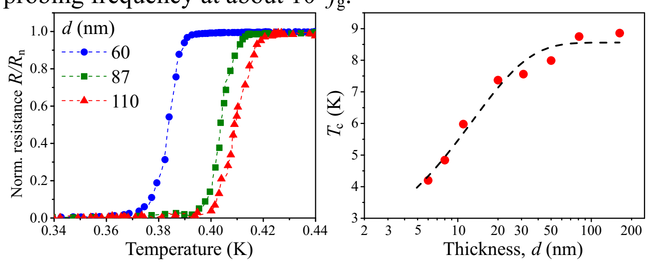

Fig. 7. The direct current $R(T)$ measured for thin films of hafnium (Hf) (left); their thermal sensitivity, TdR/RdT ≈ 50, is below the limit of 200 at $f = 10^{-2}f_g$ (see Fig. 2). Dependence $T_c(d)$ shows reduction of T_c for thin films of Nb deposited on sapphire (dashed line is the exponential fit) (right).

This article has been accepted for publication in a future issue of this journal, but has not been fully edited. Content may change prior to final publication. Citation information: DOI 10.1109/TASC.2017.2655507, IEEE Transactions on Applied Superconductivity

IV. Discussion

A. Optical system corrections

Adjusting a Gaussian-beam optical system at submillimeter wavelength is a serious engineering task, especially for a window-cryostat system. Since it was hard to expect high coupling efficiency, we compared the power received from the calibrated terahertz CW-source at *fixed bath temperature* (see Fig. 8) for known thermal conductance, G_T. The value $G_T \approx 140$ nW/K was obtained using the isothermal technique [15] for witness bridges of the same size as the bridge in the resonator. The resulting beam efficiency is found to be ~5%, and NET from Fig. 5b can be corrected for the value better than 0.1K/√Hz. Since NEP =NET×k_B×BW is related to the input bandwidth, the NEP ~10^{-13} W/√Hz can be estimated for the input BW=100 GHz.

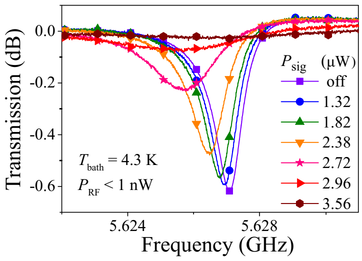

Fig. 8. Experimental data used to evaluate the optical coupling efficiency of the quasi-optical detector. The calibrated THz power alone affects the Q-factor since the probing power is very low (no crater). A transmittance of 5% was estimated using a known value of G_T.

B. Stability and gain

The regime of operation for an RFTES can be found as the graphical solution illustrated in Fig. 9 (left). This solution is based on balancing the power dissipated in the device with the power going into the heat sink, $P_{dis}(R(T), R_s)=G_T(T-T_{bath})$, which gives one or two cross-line solutions. The different temperature points, T_{bath}, are illustrated with $R(T)$ in Fig. 3 (right). It is worth adding here that, following the data from Fig. 9, the stable regimes can be available for $\delta|S_{31}|^2(\delta R) > 0$, although the negative ETF cannot be present due to $R/R_S < 1$. The low R allows for the (infinite) gain, as discussed above. This conclusion can be supported with the solutions of equation $|S_{21}|^2 = f(R(T), R_s)$ for R using experimental curves from Fig. 4 as shown in Fig. 9 (right). The presence of the essential gain may explain the fact from [7] that the measured NEP was surprisingly insensitive to changes in configuration of the amplification channel.

A complex spectrum of the output microwave signal was found in the experiment (Fig. 10); it can be evaluated as a small (-40 dBc) pulsed modulation of the input microwave signal limited to within the bandwidth of the resonator. We believe this modulation could be due to an interplay between recovery times of the microwave current and the RF-current-driven dissipative hopping of thermally activated vortices in the superconducting part of the micro-bridge [16]. At higher values P_{RF}, the resistive domain in the micro-bridge becomes larger, the Q-factor decreases and the RF-current recovers faster after a vortex-hopping event. Thus, the time between vortex-hopping events is shortened, which widens the observed spectrum.

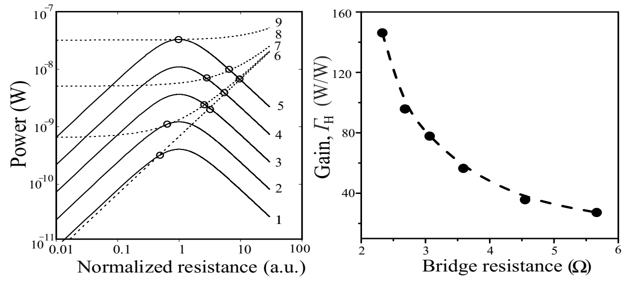

Fig. 9. Graphical solution for operational points as the balance of the coupled power P_{RF}~S_{31} (solid curves 1-5) and the sinked power (dashed curves 6-9) vs R/R_S for different bath temperatures; $T_6 \approx T_c$, $T_9 < T_c$ as in Fig. 3; circles denote cross-points of the stable balance (left). The gain, Γ_H, evaluated from Fig. 4; all data on Γ_H are for $R/R_S < 1$, i. e. for the case of $\delta|S_{31}|^2(\delta R) > 0$; $R_S \approx 8$ Ohm is derived from Fig. 4 using EM-modeling (right).

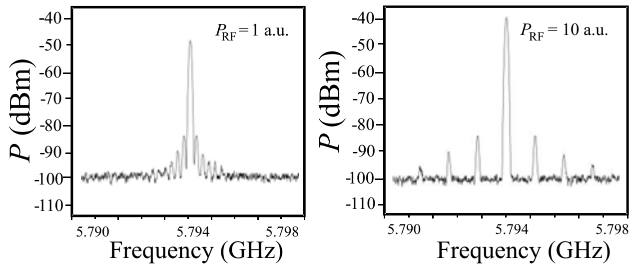

Fig. 10. Output spectra for RFTES operated at 1.5 K for two levels of probing signal: P_{RF} = 1 a.u. (left) and P_{RF} = 10 a.u. (right). Spectra are typical for pulsed modulation; bandwidth varies 3 times meaning drop of the Q-factor; modulation is arbitrarily low (-40 dBc).

V. Conclusion

We presented recent progress in both the development and understanding of a terahertz-range RFTES detector at liquid ^{4}He temperatures by demonstrating a single-pixel detector at 6 GHz and a 7-pixel FDM-array at about 8 GHz. The detector with transition temperature $T_c \approx 5.3$ K exhibits temperature sensitivity NET~0.1 K/Hz$^{1/2}$ (corrected for optical loss) at 4.5 K bath temperature, promising NEP~10^{-13} W/√Hz. Clear evidence of negative electro-thermal feedback was observed for resonances in the range of 5.6-8.2 GHz. A parasitic spectrum of pulsed modulation was discovered that may contribute to the NEP of the Nb demonstrator. The modulation amplitude is small (-40 dBc), and we attribute it to thermally activated vortex-hopping events in the micro-bridge. We believe, it will be possible to avoid this effect by operating at temperatures below 1 K. RFTES devices made with hafnium films ($T_c \approx 0.4$ K) should allow for operating in a regime where quasiparticles in the micro-bridge are more thermally isolated.

Acknowledgment

The authors acknowledge Nikolay Abramov and Eugen Erhan for their help in the experimental study.

References

[1] T. M. Lantinga, Hsiao-Mei Choa, John Clarke, Matt Dobbs et al., “Frequency domain multiplexing for large-scale bolometer arrays,”

Millimeter and Submillimeter Detectors for Astronomy, vol. 4855, pp. 172-181, 2003.

[2] P. K. Day, H. G. LeDuc, B. A. Mazin, A. Vayonakis, J. Zmuidzinas. "A broadband superconducting detector suitable for use in large arrays "Nature, 425, 817 (2003).

[3] K. D. Irwin, G. C. Hilton, "Transition-edge sensors," *Topics in Applied Physics,* vol. 99, pp.63-149, 2005.

[4] Wayne Holland, Michael MacIntosh, Alasdair Fairley et al., "SCUBA-2: a 10,000-pixel submillimeter camera for the James Clerk Maxwell Telescope," in *Proc. of the SPIE*, vol. 6275, p. 62751E, 2006.

[5] S. V. Shitov, "Bolometer with high-frequency readout for array applications," *Technical Physics Letters*, vol. 37, pp. 932–934, 2011.

[6] A. Kuzmin, S. V. Shitov, A. Scheuring, J. M. Meckbach, K. S. Il'in, S. Wuensch, A. V. Ustinov, M. Siegel, "Development of TES bolometers with high-frequency readout circuit," *IEEE Transactions on Terahertz Science and Technology*, 2013. DOI: 10.1109/TTHZ.2012.2236148 .

[7] S. V. Shitov, N. N. Abramov, A. A. Kuzmin, M. Merker, M. Arndt, S. Wuensch, K. S. Ilin, E. V. Erhan, A. V. Ustinov, M. Siegel, "Wide-Range Bolometer with RF Readout TES," *IEEE Trans. Appl. Supercond.* 12/2014; 25(3). DOI:10.1109/TASC.2014.2385090

[8] C.J. Gorter and H.B.G. Casimir, Physik. Z. 35, 963 (1934); Z. Physik 15, 539 (1934)

[9] D. C. Mattis and J. Bardeen, "Theory of the Anomalous Skin Effect in Normal and Superconducting Metals", *Phys. Rev.* vol. 111, p. 412, 1958.

[10] B. S. Karasik, W. R. McGrath, M. E. Gershenson, A. V. Sergeev, "Photon-noise-limited direct detector based on disorder-controlled electron heating," *J. Appl. Phys.* 87, 7586, 2000.

[11] B. S. Karasik, S. V. Pereverzev, D. Olaya, J. Wei, M. E. Gershenson A. V. Sergeev, "Noise measurements in hot-electron titanium nanobolometers," *IEEE Trans. Terahertz Sci. Tech.,* 19, pp. 532-535 2009.

[12] A.V. Gurevich, R.G. Mints, "Self-heating in normal metals and superconductors" Rev. Mod. Phys., 59, 941–999, (1987).

[13] A. Luukanen and J. P. Pekola, "A superconducting antenna-coupled hot-spot microbolometer", *Appl. Phys. Lett.,* 82, 3970 (2003).

[14] E. M. Gershenzon, M. E. Gershenzon, G. N. Gol'tsman, A. M. Lyul'kin, A. D. Semenov, A. V. Sergeev, "Electron-phonon interaction in ultrathin Nb films," *Sov. Phys. JETP*, vol. 70, no. 3, pp.505–511, 1990.

[15] H. Ekström, B.S. Karasik, E. Kollberg and K.S. Yngvesson,"Conversion gain and noise of niobium superconducting hot-electron-mixers" *IEEE Trans Microw. Theory Tech*. 43 938, (1995).

[16] H. Bartolf, A. Engel, A. Schilling, K. Il'in, M. Siegel, H.-W. Hübers, A. Semenov, "Current-assisted thermally activated flux liberation in ultrathin nanopatterned NbN superconducting meander structures", *Phys. Rev. B* 81, 024502, (2010).